Interfacial effects on the spin density wave in FeSe/$SrTiO_3$ thin films

Hai-Yuan Cao,[1] Shiyong Tan,[1,2] Hongjun Xiang,[1] D. L. Feng,[1,2] and Xin-Gao Gong[1]

[1]*State Key Laboratory of Surface Physics, Key Laboratory for Computational Physical Sciences (MOE), Department of Physics, Fudan University, Shanghai 200433, China*

[2]*Advanced Materials Laboratory, Fudan University, Shanghai 200433, China*

(Received 14 October 2013; revised manuscript received 16 December 2013; published 6 January 2014)

Recently the signs of both superconducting transition temperature (T_c) beyond 60 K and spin density wave (SDW) have been observed in FeSe thin film on $SrTiO_3$ (STO) substrate, which suggests a strong interplay between superconductivity and magnetism. With the first-principles calculations, we find that the substrate-induced tensile strain tends to stabilize the collinear antiferromagnetic (CAF) state in FeSe thin film by enhancing of the next-nearest-neighbor superexchange antiferromagnetic interaction bridged through Se atoms. On the other hand, we find that when there are oxygen vacancies in the substrate, the significant charge transfer from the substrate to the first FeSe layer would suppress the magnetic order there, and thus the high-temperature superconductivity could occur. In addition, the stability of the CAF state is lowered when FeSe is on a defect-free STO substrate due to the redistribution of charges among the Fe 3*d* orbitals. Normally heavy electron doping would kill superconductivity as it suppresses the spin fluctuations as well, but the expanded lattice constants in this system enhance the magnetism and thus preserve the superconductivity. Our results provide a comprehensive microscopic explanation for the recent experimental findings, and build a foundation for the further exploration of the superconductivity and magnetism in this superconducting interface.

DOI: 10.1103/PhysRevB.89.014501 PACS number(s): 74.70.Xa, 68.35.−p, 74.78.−w, 75.30.Fv

I. INTRODUCTION

Magnetism always seems to be involved in the superconducting mechanism of high-T_c superconductors. Often the superconductivity occurs when the long-range magnetic order is suppressed somehow, and yet there are underlying spin fluctuations and antiferromagnetic (AFM) interactions that could mediate the Cooper paring of the electrons [1]. Recently a large superconducting gap in monolayer FeSe thin film grown on STO substrate was observed by both scanning tunneling spectroscopy (STS) [2] and angle-resolved photoemission spectroscopy (ARPES) [3–5], with the superconducting transition likely at 65 K. This would establish a new T_c record for the iron-based superconductors. Intriguingly it is well known that the bulk FeSe only exhibits a T_c around 8 K [6,7], or 37 K under compressional pressure [8]. It is thus remarkable to observe a higher T_c in monolayer FeSe on STO, which is under the tensile strain imposed by the substrate.

For FeSe bulk material and thin film, a collinear 2×1 SDW (also known as CAF state) order is theoretically predicted to be the ground state, similar to that in the iron pnictides [9–12]. Tan *et al*. have substantiated the presence of spin density wave (SDW) in multilayer FeSe thin films which were grown layer by layer on the STO substrate with molecular beam expitaxy, and they showed that when the tensile strain decreases as the lattice relaxes with increasing thickness, the strength of the SDW decreases as well [4]. To our knowledge, no previous theoretical study has been focused on the evolution of the magnetism with the lattice constant in this system. According to the strong interplay between superconductivity and magnetism, the study on how the interfacial effect influences the magnetism in FeSe/STO thin film should be helpful for the understanding of the superconductivity there.

The SDW would have been the most prominent in monolayer FeSe next to the STO due to the most pronounced strain from the substrate, had it not been suppressed by the charge transferred from the oxygen-vacant substrate, as suggested by both the experiment [4] and theory [13]. However, previous theoretical studies were not conclusive. Liu *et al*. analyzed the orbital-resolved partial density of states (PDOS) from the density functional theory (DFT) calculations, and did not find substantial charge transfer between FeSe and the STO substrate [11]. On the other hand, Zheng *et al*. predicted a considerable charge transfer from surface O atoms of STO substrate to Fe atoms of the FeSe monolayer [14]. Another recent theoretical paper excluded the Se vacancy in FeSe as the source of electron doping for superconductivity [15], which further indicates that the oxygen vacancy on the STO substrate should play an indispensable role in the Fe-HTS. For these reasons, it is necessary to further investigate how the STO substrate and the oxygen vacancies there influence the magnetic order in the monolayer FeSe.

In this paper, based on DFT calculations, we reveal how the strain, the interfacial coupling, and the oxygen-vacant STO substrate affect the magnetism in the FeSe thin film. We find the strain could enhance the Fe-Se-Fe superexchange by increasing the Fe-Se-Fe bond angle. With the increasing superexchange interaction, the local AFM exchange interaction would be enhanced. The interaction between the STO substrate and the monolayer FeSe would reduce the charge density in the spin-majority d_{xz}/d_{yz}-orbital states of the Fe atoms, which suppresses the effect of superexchange and reduces the stability of CAF state in the monolayer FeSe. If the oxygen vacancies exist on the surface of STO substrate, a certain amount of charge would be transferred from the substrate to the spin-minority d_{xz}/d_{yz}-orbital states of the Fe atoms in the monolayer FeSe, which would suppress the CAF state and allow the superconductivity to occur. Meanwhile, the original symmetry of spin configuration in monolayer FeSe would also be disturbed due to the oxygen vacancies on the substrate. All of our results are in close agreement with the recent experiment [4]. It thus provides

a detailed microscopic understanding of the interfacial effects in this intriguing system. More importantly, our results suggest that the high T_c in the monolayer FeSe is closely related to the large underlying superexchange interactions caused by its expanded lattice, which again highlight the pivotal role of magnetism in the high temperature superconductivity of iron-based superconductors. This could be the very key issue behind all the iron-based superconductors with only an electron Fermi surface, such as the electron doped monolayer FeSe and $K_xFe_2Se_2$. Normally heavy electron doping would kill superconductivity as it suppresses the spin fluctuations as well, but the expanded lattice constants in these materials enhance magnetism and thus preserve the superconductivity.

II. METHODS

To study how the substrate affects the monolayer FeSe grown on STO (001) surface, we carry out the spin-polarized first-principles calculations using the project augmented wave pseudopotential [16,17] implemented in the VASP code [18,19]. We employ the generalized gradient approximation (GGA) of Perdew-Burke-Ernzerhof for the exchange-correlation-potentials [20]. The kinetic energy cutoff of the plane-wave basis is chosen to be 400 eV. The force on all relaxed atoms after the optimization is smaller than 0.01 eV/Å. A $6 \times 6 \times 1$ k-point mesh [21] for the Brillouin zone sampling and a width of 0.1 eV for the Gaussian smearing are adopted. In all the calculations we employ a local Coulomb repulsion GGA + U approach for Ti $3d$ electrons with $U_{\mathrm{Ti}} = 2$ eV [22–24]. The electric field induced by the asymmetric relaxed STO is compensated by a dipole correction [25]. We also use the $J_1 - J_2$ Heisenberg model to describe the magnetic interactions, while the exchange parameters are fitted to the total energy of the first-principle calculations.

As shown in Fig. 1(a), we use the $2 \times 2 \times 1$ supercell to describe the magnetic order of the monolayer and bulk FeSe.

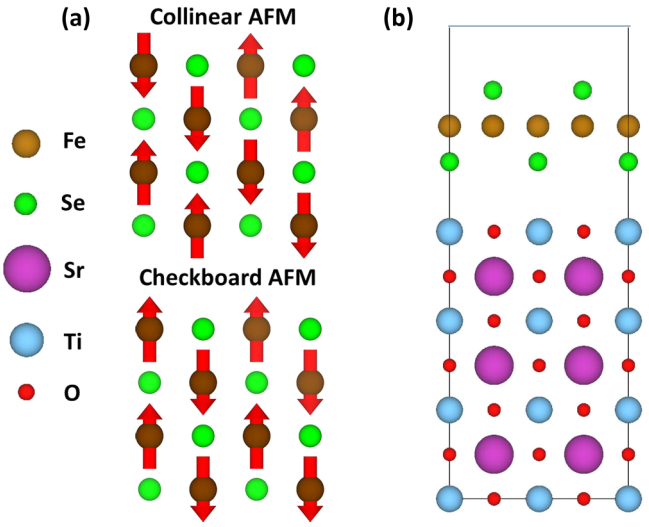

FIG. 1. (Color online) (a) Top view of atomic structures of a 2×2 supercell monolayer FeSe and spin patterns of Fe in the AFM state and the CAF state. (b) Side view of an atomic structure of a monolayer FeSe on a TiO_2 terminated STO (001) surface.

To model the interface with monolayer FeSe on STO, we use a seven-layer STO (001) slab with the 2×2 monolayer FeSe supercell on the top side plus a vacuum layer of about 10 Å as shown in Fig. 1(b). According to previous results [11], the most stable interfacial configuration is the monolayer FeSe on the TiO_2 terminated STO surface. In the present calculation, we fix the lattice constant a to be 3.905 Å, the lattice constant of the bulk STO [26]. In the structural optimization, the top two layers of STO substrate and all FeSe atoms are allowed to relax, while the atoms in the bottom layers of STO substrate are fixed at their bulk positions. To study the effect of the oxygen vacancies on the STO substrate, we choose one, two, and four vacancies out of eight oxygen atoms on the 2×2 supercell of TiO_2 terminated surface, corresponding to 12.5%,25%, and 50% vacancy concentration, respectively.

III. RESULTS AND DISCUSSION

For both free-standing FeSe and epitaxial monolayer FeSe on STO substrate, we have calculated four magnetic states, including the nonmagnetic state (NM state), the ferromagnetic state, the checkboard AFM state (AFM state), and the collinear AFM state (CAF state). The spin texture of the AFM state and the CAF state in FeSe are shown in Fig. 1(a) [10,11], respectively. By calculating and comparing the energy difference between these four states, we find that the ground state is the CAF state with a large magnetic moment of $\sim 2.4 \mu_B$ on each Fe atom for both free-standing FeSe and epitaxial FeSe on STO. The ferromagnetic state has very high energy, ~0.2 eV per Fe atom higher than the NM state, so we ignore the ferromagnetic state in the following discussions. This has also been proved in the previous theoretical studies [11,12].

First, we calculate the Fermi surface of bulk FeSe, the obtained result shown in Fig. 2(a) is in close agreement with previous calculations [9] which is composed of several hole pockets around the Γ point and two electron pockets around the M point. For the Fermi surface of the monolayer FeSe on STO substrate with lattice constant 3.905 Å, as shown in Fig. 2(b), we shift the Fermi level according to the 0.12 e^- per Fe atom as suggested by the experiment [4]. It is in good agreement with that observed in the ARPES experiments [3–5] which is

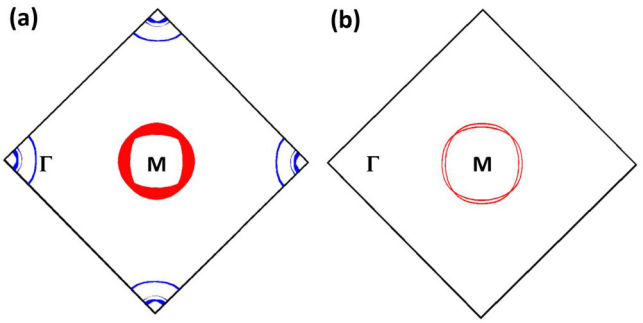

FIG. 2. (Color online) The calculated Fermi surface of (a) bulk FeSe and (b) monolayer FeSe on STO substrate. The center is M point and the corner is Γ point. The electron pockets are denoted as red while the hole pockets are denoted as blue. The hole pockets are absent in the Fermi surface of monolayer FeSe on STO substrate [3–5].

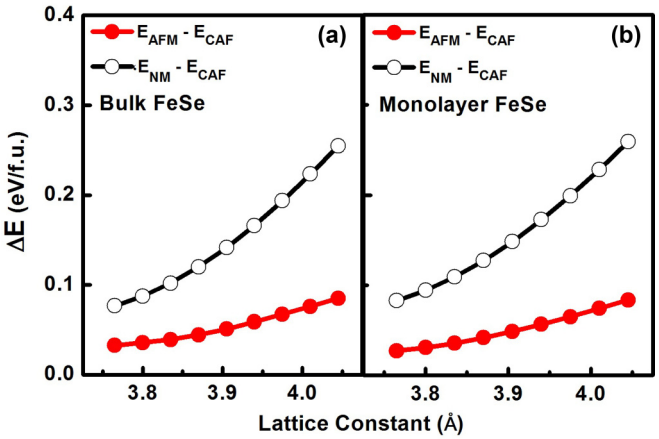

FIG. 3. (Color online) The calculated energy difference (relative to the CAF state) of the AFM state (red circle) and the NM state (black circle) versus the lattice constant of FeSe, (a) for bulk FeSe and (b) for monolayer FeSe, respectively. In both the bulk and monolayer FeSe, the CAF state tends to be energetically more stable with increasing lattice constant.

composed of two nearly degenerate electron pockets around the M point and the hole pockets around the Γ point are absent. These results confirm that our method can well reproduce the electronic structures for both bulk FeSe and monolayer FeSe on STO substrate observed in experiments.

A. How the tensile strain affects the CAF state in FeSe

We first study how the external strain could affect the stability of the CAF state. We use the energy difference between the CAF state and other two states, the AFM state and the NM state, to assess the stability of the CAF state [10,11]. In Fig. 3 we can see that the energy difference relative to the CAF state increases with the expanding of lattice constant, which indicates that the tensile strain can enhance the stability of the CAF state in both bulk and monolayer FeSe. Moreover, the energy difference in the monolayer and bulk FeSe with the same lattice constant is almost the same, therefore the relative stability of the CAF state is insensitive to the thickness of the FeSe, but sensitive to the lattice constant. Our results demonstrate that only the tensile strain rather than the thickness of the thin film can enhanced the CAF state.

To investigate why the tensile strain can affect the stability of the CAF state, we would model the magnetic interaction in FeSe with a different lattice constant. We assume that the interaction between the Fe spins dominates the energy difference between different magnetic orders. We could map the magnetic interaction to the following Heisenberg model which is described by the nearest-neighbor and next-nearest-neighbor coupling parameters J_1 and J_2 [12]:

$$H = J_1 \sum_{\langle ij \rangle} \vec{S}_i \cdot \vec{S}_j + J_2 \sum_{\langle\langle ij \rangle\rangle} \vec{S}_i \cdot \vec{S}_j, \qquad (1)$$

whereas $\langle ij \rangle$, $\langle\langle ij \rangle\rangle$ denote the summation over the nearest-neighbors and the next-nearest-neighbors, respectively. Using the method proposed by previous theoretical work [27], we can determine the value of J_1 and J_2. In bulk FeSe, we find

TABLE I. Structural parameters, calculated nearest-neighbor, and next-nearest-neighbor coupling parameters of monolayer FeSe. The definition of the Fe-Se-Fe angle is shown in Fig. 4(b). Here we assume $S = 1$ for Fe atoms.

Lattice Constant (Å)	J_1 (meV)	J_2 (meV)	J_2/J_1	Fe-Se-Fe Angle
3.765	74	43	0.58	105°
3.905	78	53	0.68	109°
4.045	82	60	0.73	113.5°

$J_1 = 74$ meV/S^2 and $J_2 = 43$ meV/S^2, in close agreement with the previous results [12].

As shown in Table I, J_1 increases only slightly with increasing lattice constant, but J_2 increases about 40% when the lattice constant increases just a few percent. More clearly, J_2/J_1 increases monotonously with lattice constant expanding, suggesting that the CAF state is getting more and more stable. According to the frustrated Heisenberg model, the magnetic exchange energy in the unit cell of FeSe with four Fe atoms is $-2J_1 + 2J_2$ for the AFM state and $-2J_2$ for the CAF state (assuming $S = 1$). It is known that the frustration between J_1 and J_2 destructs the stability of the AFM state and induces the CAF state when $J_2 > J_1/2$ for a square lattice [12].

To explore the origin of the changing of J_1 and J_2 with the lattice constant, we have calculated the charge distribution around Fe and Se atoms. As shown in Figs. 4(a) and 4(b), there is almost no charge density between two nearest-neighbor Fe atoms but the bonds are formed between Fe and Se

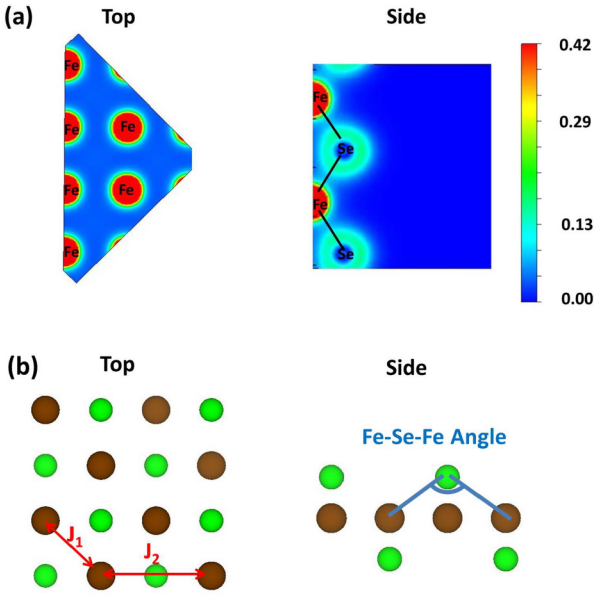

FIG. 4. (Color online) (a) The top view and the side view of the charge distribution in monolayer FeSe. In the top view, there is almost no bond between Fe atoms. In the side view, we can clearly observe that there exists a bond (black line) between Se and Fe. (b) The top view of the nearest as well as the next-nearest magnetic exchange interacting J_1 and J_2 (red arrow) and the side view of the defined Fe-Se-Fe angle between two next-nearest Fe atoms (blue line).

atoms. Similar to the previous calculation of LaFeAsO, J_2 is dominated here by the superexchange bridged by Se atoms [27,28]. According to the mechanism of superexchange and the band structure of FeSe, we find that the superexchange interaction is from the half-filled Fe d_{xz}/d_{yz} orbitals bridged by the Se p orbitals, and Goodenough-Kanamori rules state that this is AFM coupling [29]. With the expanding of the lattice constant, the out-of-plane height of Se atoms tends to decrease and the Fe-Se-Fe angle [defined in Fig. 4(b)] tends to increase as shown in Table I. The increase of the Fe-Se-Fe angle increases the overlapping of the Fe d_{xz}/d_{yz} orbitals and Se p orbitals, while the Fe-Se-Fe superexchange interaction would be maximized if the Fe-Se-Fe angle is 180° according to Goodenough-Kanamori rules [29]. From the above discussions, we can conclude that the tensile strain enhances the superexchange interaction and then enlarges the next-nearest-neighbor coupling J_2, which directly stablizes the CAF state in monolayer and bulk FeSe. Our results build the bridge between the magnetic orders and the local atomic structure, which could be tuned by tensile strain induced by the substrate.

The recent experiment by Tan *et al*. used the band separation at M point to characterize the strength of the CAF state in FeSe thin films. The observed band separation increases with expanding of the lattice constant, which is essentially caused by the different band dispersions along the AFM and FM directions in the CAF state [4]. Here we observe a linear relation between our calculated relative stability of the CAF state and the experimental band separation as shown in Fig. 5. It indicates that our calculation results of the energy difference is closely correlated to the experimental observation, and it further implies that the band separation is a relevant energy scale to characterize the strength of the CAF state in FeSe thin films. This relation with the lattice constant is directly ascribed to the enhancement of the next-nearest superexchange interaction due to the increased Fe-Se-Fe angle with the lattice expansion. Recent theoretical work predicts that a strong next-nearest AFM interaction could lead to a high temperature superconductor [1]. According to this prediction, our result shows that strain enhanced superexchange interaction should play an important role in the over 60 K high temperature superconductivity observed in FeSe-STO.

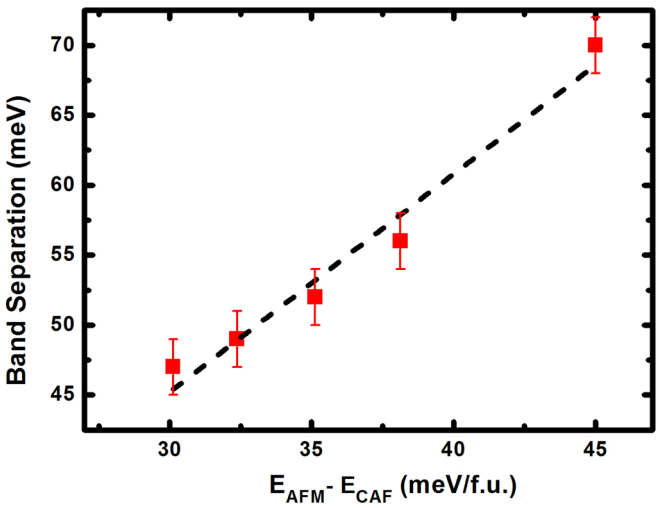

FIG. 5. (Color online) The experimental band separations for FeSe films at various lattice constants [4] versus the calculated energy difference between the AFM state and the CAF state. The dashed line is a linear fitting. The error bar for the experimental band separations is ±2 meV.

B. How the interfacial coupling affects the CAF state in FeSe

For the monolayer FeSe on a defect-free STO substrate, we did not find an apparent charge transfer at the interface from Bader analysis [30], and we did not yet find any obvious structural distortion occurring in monolayer FeSe. However, after detailed calculations of the charge difference between the epitaxial and free-standing monolayer FeSe, we find that the interfacial coupling would induce the redistribution of the charge density in epitaxial monolayer FeSe, which would decrease the charge density in the spin-majority d_{xz}/d_{yz}-orbital states of Fe atoms as shown in the inset of Fig. 6. If we gradually increase the interface distance from the equilibrium position 3.1 to 5.6 Å, the energy difference between the CAF state and the AFM state rises from 37 to 52 meV/f.u. as shown in Fig. 6. In the meantime, the charge redistribution occurring in monolayer FeSe becomes smaller and smaller, which suggests that the charge redistribution is attributed to the interfacial interaction. The decrease of the charge density in the spin-majority d_{xz}/d_{yz}-orbital states with decreasing interface distance would reduce the charge overlapping between the Fe d_{xz}/d_{yz} orbitals and the Se p orbitals, and then lower the

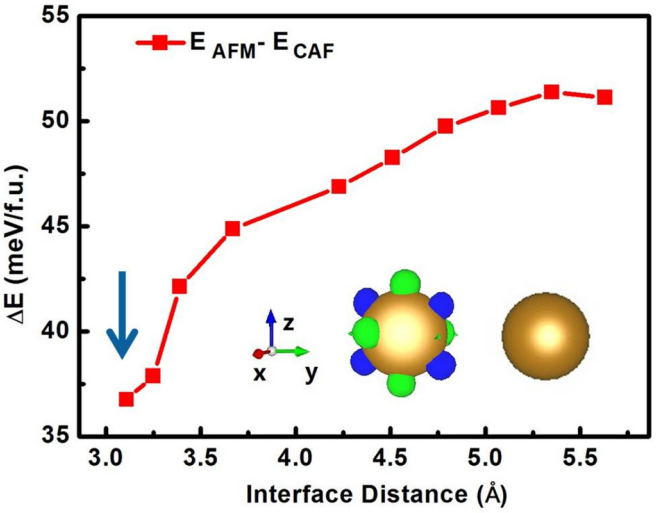

FIG. 6. (Color online) The calculated energy difference between the CAF state and the AFM state as a function of the interface distance. With the decrease of the interface distance, the CAF state becomes less stable relative to the AFM state. The blue arrow shows the equilibrium distance as 3.1 Å. Inset shows the charge redistribution on Fe atoms in epitaxial FeSe at the equilibrium distance (left side). The blue part represents the charge density lost while the green part represents the charge density gained. The inset also shows there is almost no charge redistribution on Fe atom if the interface distance is 5.6 Å (right side).

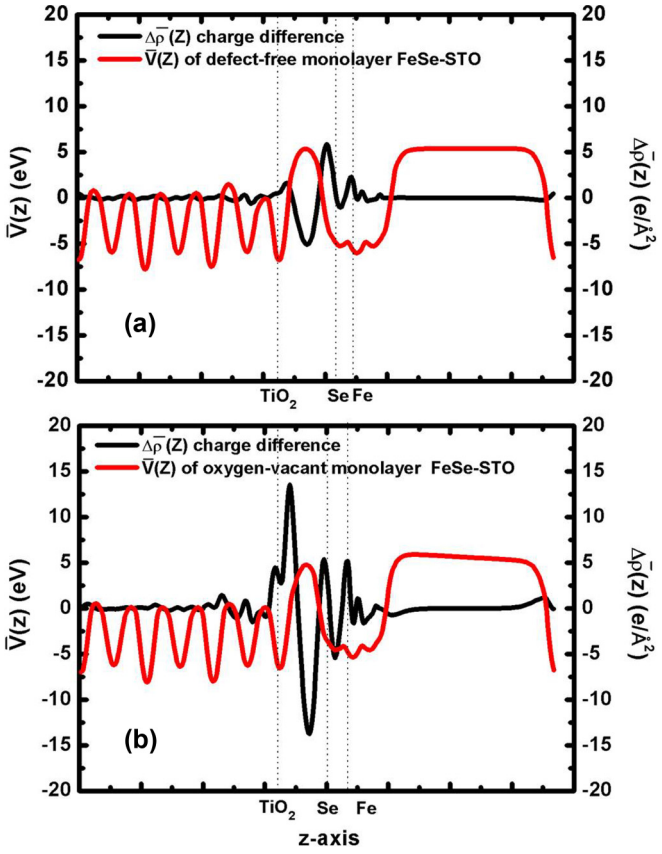

FIG. 7. (Color online) The plane-averaged charge density difference (black line) and the local potential (red line) for (a) the monolayer FeSe/defect-free STO interface and (b) the monolayer FeSe/oxygen-vacant STO interface. The position of the surface TiO_2 layer of STO substrate and FeSe atomic layers are denoted by the dotted vertical lines. Significant charge transferred from the top TiO_2 layer of the oxygen-vacant STO substrate to the Fe atomic layer can be observed here.

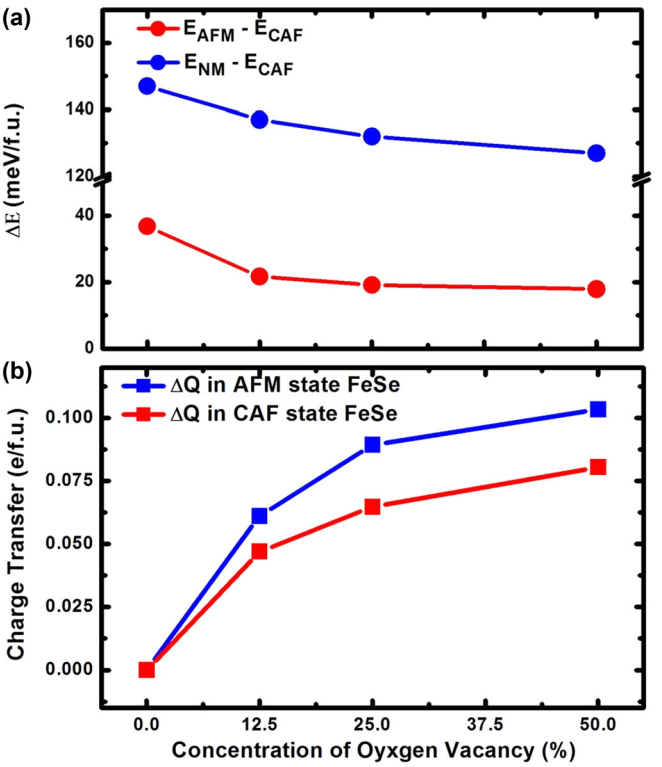

FIG. 8. (Color online) (a) The energy difference between the AFM state (blue circle), the NM state (red circle), and the CAF state with different concentration of oxygen vacancy. (b) The charge transferred to a 2×2 supercell of monolayer FeSe with the AFM state (blue square) and the CAF state (red square) calculated by Bader analysis. The charge of monolayer FeSe on defect-free STO substrate is set to be the reference. Both the oxygen vacancy and the charge transferred from STO are related to decrease the relative stability of the CAF state.

superexchange interaction. As we have discussed in Sec. III A, a smaller superexchange interaction would bring about the weaker next-nearest-neighbor coupling J_2, and degrade the stability of the CAF state in FeSe. So the interfacial interaction between monolayer FeSe and STO substrate could decrease the stability of the CAF state.

We find that the change of the d_{xz}/d_{yz}-orbital states could be induced by the dipolar field along the direction perpendicular to the interface. The plane-averaged charge density difference between the monolayer FeSe-STO, free-standing monolayer FeSe and STO substrate are shown in Fig. 7(a). Although there is no charge transfer between the monolayer FeSe and the STO substrate, the charge redistribution near the interface can be observed clearly. It forms a charge dipole at the interfacial region due to the interfacial coupling, which has been previously explained by the metal-insulator band alignment [31,32]. The interfacial dipole formed at the monolayer FeSe-STO interface could induce the electric field along the direction perpendicular to the interface which induces the change of the d-orbital order of the Fe atom. Our results demonstrate the excess electron doping to the monolayer FeSe should not come from the defect-free STO substrate. On the other hand, we propose a mechanism that the interfacial dipole field could suppress the CAF order without the apparent charge transfer.

C. How the oxygen vacancy affects the CAF state in FeSe

Oxygen vacancy on the STO surface is experimentally unavoidable due to the heat treatment in preparing the STO substrate [2]. In order to understand how the oxygen vacancy affects the property of monolayer FeSe, we have simulated monolayer FeSe on STO substrate with a different concentration of oxygen vacancies.

First, we calculate the energy difference between the NM state, the AFM state, and the CAF state, as well as the charge density distribution in monolayer FeSe on the STO substrate with different concentration of oxygen vacancies. The results are shown in Fig. 8. We find that the oxygen vacancy can induce charge transfer from the STO substrate to monolayer FeSe, the higher concentration of the oxygen vacancy, the more the charge is transferred [Fig. 8(b)]. As more and more charge transferred to the monolayer FeSe, the stability of the CAF state relative to the AFM state and the NM state decreases monotonously [Fig. 8(a)]. We also calculate the

TABLE II. Calculated nearest-neighbor and next-nearest-neighbor coupling parameters of the free-standing monolayer FeSe, monolayer FeSe on defect-free STO, and monolayer FeSe on 12.5% oxygen-vacant STO. Here we assume $S = 1$ for Fe atoms.

	J_1 (meV)	J_2 (meV)	J_2/J_1
Free-standing monolayer FeSe	82	60	0.73
Monolayer FeSe on defect-free STO	76	48	0.63
Monolayer FeSe on 12.5% oxygen-vacant STO	59	35	0.59

plane-averaged charge difference obtained by subtracting the valence charge densities of the free-standing FeSe layer and isolated STO substrate from the monolayer FeSe on STO. The results presented in Fig. 7(b) clearly show the monolayer FeSe on STO substrate with oxygen vacancies inducing significant charge transferred to Fe atoms while almost no charge transfer exists when it is on the defect-free STO substrate as shown in Fig. 7(a).

We find that the charge is transferred from the substrate to the spin-minority d_{xz}/d_{yz}-orbital states of the Fe atom in monolayer FeSe, so it would decrease the superexchange interaction and reduce the stability of the CAF state. From Table II we find J_2 decreases from 48 to 35 meV and J_2/J_1 decreases from 0.63 to 0.59 if 12.5% oxygen vacancy exists on the surface of the STO substrate. Based on the PDOS of Fe atom on STO substrate with 12.5% oxygen vacancy, we do find that about ~0.1 charge transferred to the spin-minority d_{xz}/d_{yz}-orbital states. Since the superexchange between two next-nearest ideally half-filled orbitals is the strongest, the increasing charge density in the spin-minority d_{xz}/d_{yz}-orbital states would decline the AFM superexchange coupling, and it would decrease the stability of the CAF state. Moreover, we find that the oxygen vacancy can magnetically polarize the nearby Ti atoms, and the magnetism of Ti atoms could also decrease the stability of the CAF state. For the concentration of 12.5% oxygen vacancies, the nearby Ti atom would possess a magnetic moment of 0.88 μ_B [23,33]. The ferromagnetism from the Ti atoms would break the symmetry of spin in monolayer FeSe, as shown in Fig. 9. The PDOS of spin-minority electrons of the Fe atom would increase a lot near the Fermi level. Our results provide the comprehensive explanation of how the oxygen vacancy on the STO substrate could help to suppress the CAF order in monolayer FeSe.

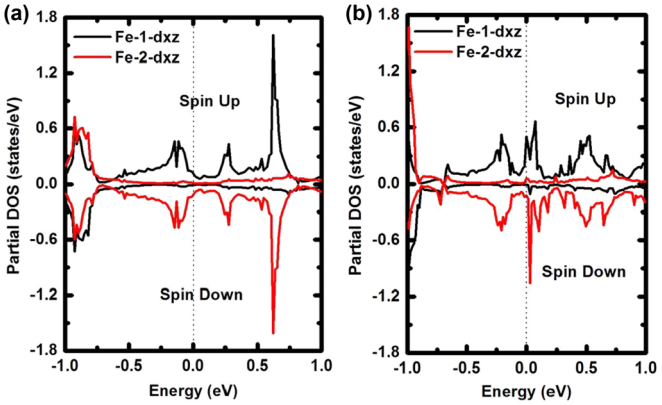

FIG. 9. (Color online) The partial density of states (PDOS) of d_{xz} orbital for two-type Fe atoms in the unit cell of the CAF state with the up-spin-majority and down-spin-majority electrons, respectively. The PDOS for Fe atoms in expitaxial monolayer FeSe on (a) the defect-free STO substrate and (b) the 12.5% oxygen-vacant STO substrate. The existence of oxygen vacancies on the surface of STO substrate disturbs the symmetry of spin of two-type Fe atoms and increases the density of states near the Fermi energy significantly for spin-minority electrons of Fe atoms.

IV. SUMMARY

We have studied the interfacial effect on the stability of the CAF state in monolayer FeSe using the GGA + U method. We find that tensile strain can increase the superexchange interaction between the next-nearest Fe atoms by increasing the Fe-Se-Fe bond angle, thus enhancing the local AFM coupling and the stability of the CAF state. However, we also find that the interfacial coupling between FeSe and STO substrate can change the charge distribution in the 3d orbitals of Fe atoms, leading to less charge density in the spin-majority d_{xz}/d_{yz} orbitals. It decreases the superexchange coupling between the next-nearest Fe atoms and suppress the stability of the CAF state. In agreement with previous calculation [13], we also observed a significant charge transferred from the oxygen-vacant substrate to monolayer FeSe. Furthermore, we find that such charge will be transferred to the spin-minority d_{xz}/d_{yz} orbitals of Fe atoms, and the almost fully occupied d_{xz}/d_{yz} orbitals will decline AFM superexchange interaction, thus will also suppress the stability of the CAF state.

In summary, the substrate induced tensile strain can enhance the next-nearest antiferromagnetic interaction, while the interfacial coupling and charge transfer will destroy the long range magnetic order. We provide a systematical microscopic description for the interfacial effects on the magnetism and further suggest a strong correlation between the magnetism and the possible high T_c in monolayer FeSe on STO substrate. Our results build the foundation for understanding the prominent role of magnetism in this new kind of iron-based superconductor. According to this understanding, we have experimentally achieved a gap closing temperature of 70 K by expanding the lattice constant [34].

ACKNOWLEDGMENTS

H.Y.C. thanks Shiyou Chen for helpful discussions. The work was partially supported by the Special Funds for Major State Basic Research, National Natural Science Foundation of China (NSFC), Program for Professor of Special Appointment (Eastern Scholar). Computation was performed in the Supercomputer Center of Fudan University.

[1] J. Hu and H. Ding, Sci. Rep. **2**, 381 (2012).
[2] Q.-Y. Wang, Z. Li, W.-H. Zhang, Z.-C. Zhang, J.-S. Zhang, W. Li, H. Ding, Y.-B. Ou, P. Deng, K. Chang *et al.*, Chin. Phys. Lett. **29**, 037402 (2012).
[3] S. He, J. He, W. Zhang, L. Zhao, D. Liu, X. Liu, D. Mou, Y.-B. Ou, Q.-Y. Wang, Z. Li *et al.*, Nat. Mater. **12**, 605 (2013).
[4] S. Tan, Y. Zhang, M. Xia, Z. Ye, F. Chen, X. Xie, R. Peng, D. Xu, Q. Fan, H. Xu *et al.*, Nat. Mater. **12**, 634 (2013).
[5] D. Liu, W. Zhang, D. Mou, J. He, Y.-B. Ou, Q.-Y. Wang, Z. Li, L. Wang, L. Zhao, S. He *et al.*, Nat. Commun. **3**, 931 (2012).
[6] F.-C. Hsu, J.-Y. Luo, K.-W. Yeh, T.-K. Chen, T.-W. Huang, P. M. Wu, Y.-C. Lee, Y.-L. Huang, Y.-Y. Chu, D.-C. Yan *et al.*, Proc. Natl. Acad. Sci. U.S.A. **105**, 14262 (2008).
[7] C.-L. Song, Y.-L. Wang, Y.-P. Jiang, Z. Li, L. Wang, K. He, X. Chen, X.-C. Ma, and Q.-K. Xue, Phys. Rev. B **84**, 020503 (2011).
[8] S. Medvedev, T. M. McQueen, I. A. Troyan, T. Palasyuk, M. I. Eremets, R. J. Cava, S. Naghavi, F. Casper, V. Ksenofontov, G. Wortmann *et al.*, Nat. Mater. **8**, 630 (2009).
[9] A. Subedi, L. Zhang, D. J. Singh, and M. H. Du, Phys. Rev. B **78**, 134514 (2008).
[10] T. Bazhirov and M. L. Cohen, J. Phys.: Condens. Matter **25**, 105506 (2013).
[11] K. Liu, Z.-Y. Lu, and T. Xiang, Phys. Rev. B **85**, 235123 (2012).
[12] F. Ma, W. Ji, J. Hu, Z.-Y. Lu, and T. Xiang, Phys. Rev. Lett. **102**, 177003 (2009).
[13] J. Bang, Z. Li, Y. Y. Sun, A. Samanta, Y. Y. Zhang, W. Zhang, L. Wang, X. Chen, X. Ma, Q.-K. Xue *et al.*, Phys. Rev. B **87**, 220503 (2013).
[14] F. Zheng, Z. Wang, W. Kang, and P. Zhang, Sci. Rep. **3**, 2213 (2013).
[15] T. Berlijn, H. Cheng, P. Hirschfeld, and W. Ku, arXiv:1307.0140.
[16] P. E. Blöchl, Phys. Rev. B **50**, 17953 (1994).
[17] G. Kresse and D. Joubert, Phys. Rev. B **59**, 1758 (1999).
[18] G. Kresse and J. Furthmüller, Phys. Rev. B **54**, 11169 (1996).
[19] G. Kresse and J. Furthmüller, Comput. Mater. Sci. **6**, 15 (1996).
[20] J. P. Perdew, K. Burke, and M. Ernzerhof, Phys. Rev. Lett. **77**, 3865 (1996).
[21] H. J. Monkhorst and J. D. Pack, Phys. Rev. B **13**, 5188 (1976).
[22] N. Pavlenko, T. Kopp, E. Y. Tsymbal, G. a. Sawatzky, and J. Mannhart, Phys. Rev. B **85**, 020407 (2012).
[23] N. Pavlenko, T. Kopp, E. Y. Tsymbal, J. Mannhart, and G. A. Sawatzky, Phys. Rev. B **86**, 064431 (2012).
[24] M. Breitschaft, V. Tinkl, N. Pavlenko, S. Paetel, C. Richter, J. R. Kirtley, Y. C. Liao, G. Hammerl, V. Eyert, T. Kopp *et al.*, Phys. Rev. B **81**, 153414 (2010).
[25] J. Neugebauer and M. Scheffler, Phys. Rev. B **46**, 16067 (1992).
[26] F. El-Mellouhi, E. N. Brothers, M. J. Lucero, and G. E. Scuseria, Phys. Rev. B **84**, 115122 (2011).
[27] F. Ma and Z.-Y. Lu, Phys. Rev. B **78**, 033111 (2008).
[28] F. Ma, Z.-Y. Lu, and T. Xiang, Phys. Rev. B **78**, 224517 (2008).
[29] J. B. Goodenough, Phys. Rev. **100**, 564 (1955).
[30] W. Tang, E. Sanville, and G. Henkelman, J. Phys.: Condens. Matter **21**, 084204 (2009).
[31] J. Tersoff, Phys. Rev. B **30**, 4874 (1984).
[32] J. Tersoff, Phys. Rev. B **32**, 6968 (1985).
[33] J. Park, B.-G. Cho, K. D. Kim, J. Koo, H. Jang, K.-T. Ko, J.-H. Park, K.-B. Lee, J.-Y. Kim, D. R. Lee *et al.*, Phys. Rev. Lett. **110**, 017401 (2013).
[34] R. Peng, X. P. Shen, X. Xie, H. C. Xu, S. Y. Tan, M. Xia, T. Zhang, H. Y. Cao, X. G. Gong, J. P. Hu *et al.*, arXiv:1310.3060.